Joint International Topical Meeting on Mathematics & Computation and Supercomputing in Nuclear Applications (M&C + SNA 2007)
Monterey, California, April 15-19, 2007, on CD-ROM, American Nuclear Society, LaGrange Park, IL (2007)

A P_1 BENCHMARK FOR TIME DEPENDENT THERMAL RADIATIVE TRANSFER

Ryan G. McClarren
Los Alamos National Laboratory*
PO Box 1663
Los Alamos, New Mexico 87545
ryanmc@lanl.gov

James Paul Holloway
Department of Nuclear Engineering and Radiological Sciences
College of Engineering
University of Michigan
2355 Bonisteel Boulevard
Ann Arbor, Michigan 48109 2104

Thomas A. Brunner
Sandia National Laboratories†
PO Box 5800, MS 1186
Albuquerque, New Mexico 87185 1186
tabrunn@sandia.gov

ABSTRACT

We present an analytic solution for time-dependent P_1 (telegrapher's equation) radiative transfer. This solution will be useful for verifying spherical harmonics based transport codes and to providing insight into the properties of the P_n equations. The solution is for a uniform, isotropic and non-scattering medium that has a heat capacity proportional to the material temperature cubed (T^3). We first derive the time-dependent Greens function for the P_1 equations in planar geometry. This result is then used to generate a P_1 solution to one of the Su-Olson problems. We also use the planar Greens function to generate the Greens function for a pulsed point source in an infinite medium. With this point source we have reduced the problem of solving the P_1 equations in a uniform medium to quadrature. The solution for a pulsed line source is developed, again because of its utility for verifying P_n based thermal radiation transport codes.

Key Words: analytic benchmarks, spherical harmonics equations, time dependent radiative transfer

1. INTRODUCTION

Solving the time dependent thermal transport equations is a difficult problem; the number of degrees of freedom is large and the system is nonlinear. These nonlinearities in the temperature variable make all but the most trivial problems tractable analytically.

*Los Alamos National Laboratory is operated by Los Alamos National Security, LLC, for the U.S. Department of Energy under contract DE-AC52-06NA25396.

†Sandia is a multiprogram laboratory operated by Sandia Corporation, a Lockheed Martin Company, for the United States Department of Energy's National Nuclear Security Administration under Contract DE-AC04-94AL85000.

Despite the difficulty of solving thermal transport problems, using a cleverly devised form of the heat capacity (C_V) as a function of temperature, it is possible to find linearized equations that can be solved. Using this form, grey diffusion solutions [1, 2] have been found for various problems. Also, using a modified P_1 and P_2 approximation for grey transport Pomraning and Shokair found the value of the radiation and temperature fields at the free-surface and the total radiation and material energies of a half-space problem [3]; Ganapol and Pomraning found these quantities for the full transport equations [4]. The transport solution for the radiation and temperature fields throughout a problem domain was found by Su and Olson [5].

One might wonder why so much ink has been spilled to solve radiative transfer problems that involve an assumed (and unrealistic[‡]) form of the heat capacity. This work has not been an exercise in solipsism but rather represents the need to have analytic solutions to verify the codes written to solve the nonlinear radiation transport equations. Given that a code should have the ability to take an arbitrary heat capacity for a material, these solutions can be used to verify numerical codes (i.e. a diffusion code should converge to the analytic diffusion solution). Furthermore, given an analytic solution to the transport equation we can test the accuracy and applicability of various approximations to the transport solution.

Below we will develop the first time-dependent P_1 (telegrapher's equation) solutions for thermal radiative transfer. We do this by first developing the Green's function for the P_1 equations and then using this solution to "build up" solutions to other problems. We were originally motivated to perform this work to verify our own spherical harmonics codes for thermal transport [7, 8].

2. THE P_1 SLAB GEOMETRY GREEN'S FUNCTION

2.1. P_1 Equations for Radiative Transfer

The one-dimensional transport equation for grey radiation in the absence of scattering is given by

$$\frac{1}{c}\frac{\partial I}{\partial t} + \mu\frac{\partial I}{\partial z} + \sigma_a I = \frac{\sigma_a acT^4}{4\pi} + S. \tag{1}$$

The equation that governs the material temperature is

$$C_v\frac{\partial T}{\partial t} = \sigma_a(c\mathcal{E} - acT^4) \tag{2}$$

where we have written the radiation energy density as

$$\mathcal{E} = \frac{2\pi}{c}\int_{-1}^{1} d\mu\, I(\mu). \tag{3}$$

The P_1 equations are obtained by taking angular moments of Eq. (1). The first of the P_1 equations (the zeroth moment of Eq. (1)) is given by

$$\frac{1}{c}\frac{\partial \mathcal{E}}{\partial t} + \frac{1}{c}\frac{\partial \mathcal{F}}{\partial z} + \sigma_a\mathcal{E} = a\sigma_a T^4 + \frac{S}{c}. \tag{4}$$

The radiation flux, $\mathcal{F}$, is the first moment of the specific intensity

$$\mathcal{F} = 2\pi\int_{-1}^{1} d\mu\, \mu I(\mu). \tag{5}$$

‡The heat capacity of a material is nearly constant as a function of temperature, except in the region where the material is ionizing [6].

The second equation in the P_1 system is found by taking the first moment of Eq. (1) and assuming that the specific intensity depends linearly on μ. This equation is given by

$$\frac{1}{c}\frac{\partial \mathcal{F}}{\partial t} + \frac{c}{3}\frac{\partial \mathcal{E}}{\partial z} + \sigma_a \mathcal{F} = 0. \tag{6}$$

To proceed we make a common [1, 2, 5] assumption on the behavior of the heat capacity of the material to make Eq. (2) linear in T^4, namely we stipulate that

$$C_v = 4aT^3. \tag{7}$$

We will normalize the P_1 system using

$$x \equiv \sigma_a z, \quad \tau \equiv \epsilon c \sigma_a t, \quad E \equiv \frac{\mathcal{E}}{aT_r^4}, \tag{8}$$

$$U \equiv \frac{T^4}{T_r^4}, \quad F \equiv \frac{\mathcal{F}}{aT_r^4}, \quad Q = \frac{S}{acT_r^4}. \tag{9}$$

Given these definitions the P_1 system becomes

$$\epsilon\frac{\partial E}{\partial \tau} + \frac{1}{c}\frac{\partial F}{\partial x} = -\left(E - U\right) + \frac{Q}{\sigma_a}, \tag{10}$$

$$\epsilon\frac{\partial F}{\partial \tau} + \frac{c}{3}\frac{\partial E}{\partial x} + F = 0, \tag{11}$$

$$\frac{\partial U}{\partial \tau} = (E - U). \tag{12}$$

The boundary and initial conditions that we will use throughout this paper are

$$E(\pm\infty, \tau) = 0, \quad E(x, 0) = U(x, 0) = 0. \tag{13}$$

2.2. Solution to Normalized P_1 Equations

We can obtain the Green's function for the system by setting the source to be $Q = \delta(x)\delta(\tau)$ (for convenience we also set $\sigma_a = 1$). After Laplace and Fourier transforming the P_1 system of equations with $\epsilon = 1$, the transformed radiation energy density is given by

$$\hat{\hat{E}}(k, s) = \frac{3(s+1)}{\sigma_a\,(k + i\Lambda)(k - i\Lambda)} \tag{14}$$

where

$$\Lambda^2 = 3s(s+2). \tag{15}$$

The form of Eq. (14) allows us to use the residue theorem and knowledge about where the poles lie to invert the Fourier transform. The inverse Laplace transform can be found with the help of an exhaustive table of Laplace transforms [9], yielding the Green's function for the radiative transfer P_1 equations with a pure absorber and $C_v = 4aT^3$

$$E(x, \tau) = \frac{\sqrt{3}}{2}e^{-\tau}\left(\frac{\tau I_1(\sqrt{\tau^2 - 3x^2})}{\sqrt{\tau^2 - 3x)^2}}h(\tau - \sqrt{3}|x|) + I_0(\sqrt{\tau^2 - 3x^2})\delta(\tau - \sqrt{3}|x|)\right). \tag{16}$$

In this equation we have denoted the modified Bessel function of the first kind of order ν with I_ν and

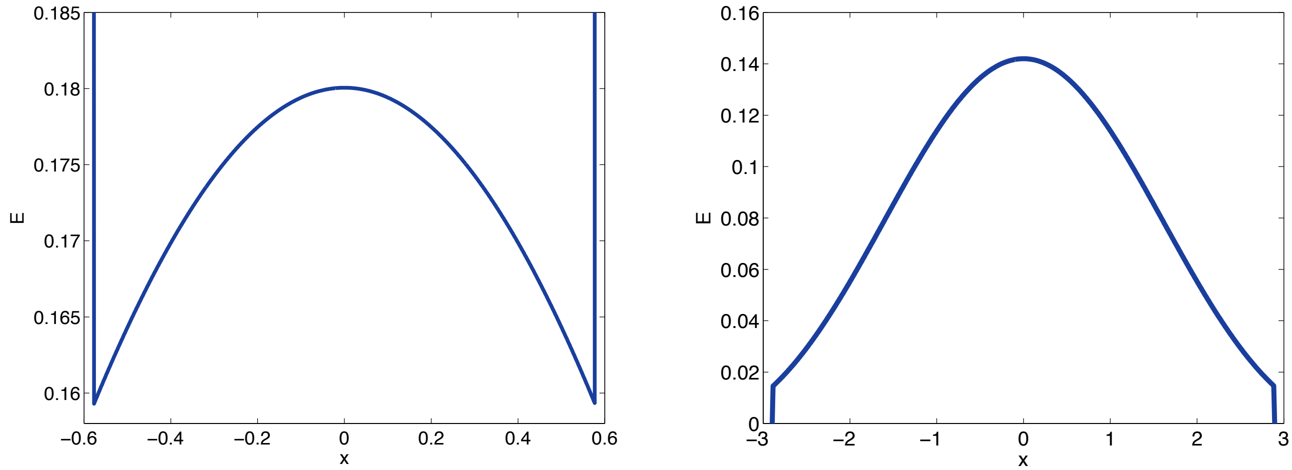

(a) $\tau = 1$

(b) $\tau = 5$

Figure 1. The Green's function solution to the P_1 equations.

the Heaviside step function by h. In the Green's function we note some important properties. The finite propagation speed allowed by the P_1 equations (due to their hyperbolic nature) is manifest in the delta and Heaviside functions; the solution has a front of uncollided source particles with a speed of $1/\sqrt{3}$ moving away from the origin, with a decaying modified Bessel function behind the front. These features can be seen in Fig. 1 which shows the Green's function solution. Early in time most of the energy is in the uncollided flux (the delta functions) and later in time a large majority of the particles have been absorbed and reëmitted and very few are still streaming straight from the source making the delta functions weak. The stength of the delta function decays as $\exp(-\tau)$, hence, most of the energy in the solution is in the reëmitted particles after a few collision times.

3. SU-OLSON BENCHMARK PROBLEM

We can use the Green's function to construct the P_1 solution to one of the Su-Olson benchmarks. This problem has a unit source in the range $|x| < 0.5$ and $\tau < 10$ with a uniform material, $\sigma_a = 1$. The initial condition has zero energy density.

To construct this solution we will change variables in Eq. (16) changing $x \to (x - y)$ and $\tau \to \tau'$, then we integrate the y variable over the source and the τ' variable from zero to τ (for $\tau < 10$). This gives the energy density for this benchmark for $\tau \leq 10$ as

$$E(x,\tau) = \frac{\sqrt{3}}{2}\int_{-0.5}^{0.5} dy \left(e^{-\sqrt{3}|x-y|} h(\tau - \sqrt{3}|x-y|) + \int_0^{\tau} d\tau' \frac{e^{-\tau'}\tau' I_1(\sqrt{\tau'^2 - 3(x-y)^2})}{\sqrt{\tau'^2 - 3(x-y)^2}} h(\tau' - \sqrt{3}|x-y|) \right), \tag{17}$$

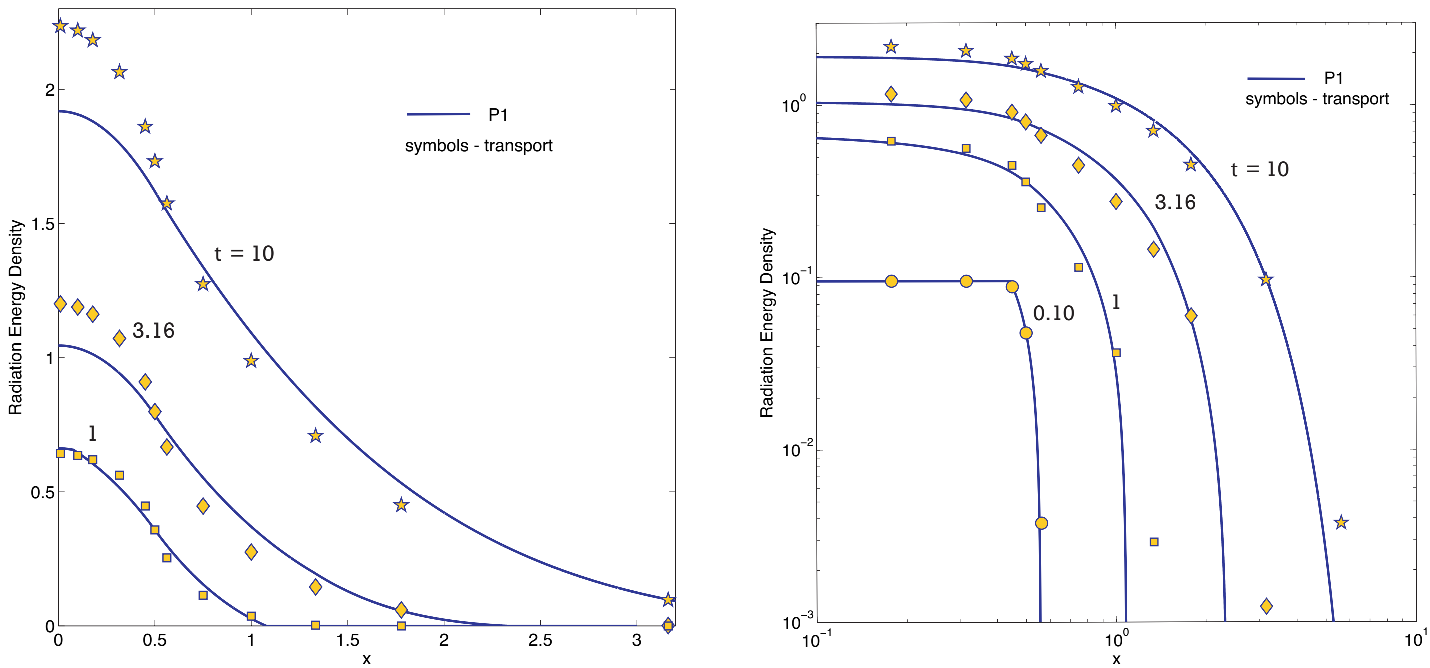

(a) Linear Scale

(b) Logarithmic Scale

Figure 2. Analytic solutions to the P_1 and transport equations for the finite source problem.

and for $\tau > 10$ as

$$E(x,\tau) = \frac{\sqrt{3}}{2}\int_{-0.5}^{0.5} dy \Bigg(e^{-\sqrt{3}|x-y|} h(\tau - \sqrt{3}|x-y|) h(10 - \tau + \sqrt{3}|x-y|) + \int_{\tau-10}^{\tau} d\tau' \frac{e^{-\tau'}\tau' I_1(\sqrt{\tau'^2 - 3(x-y)^2})}{\sqrt{\tau'^2 - 3(x-y)^2}} h(\tau' - \sqrt{3}|x-y|) \Bigg). \quad (18)$$

This function can be computed and plotted using Mathematica in a straightforward manner. In Figs. 2(a) - 2(b) we plot the P_1 analytic solution along with the transport solutions presented in Ref. 5.

These results show how applicable the P_1 approximation is on this particular problem. The P_1 solution agrees well with the transport solution early in time, but at later times the P_1 solution is too low in and near the source region and too high away from the source. Furthermore, the on the logarithmic scale (Fig. 2(b)) we can see the effect of the slow P_1 wavespeed: the P_1 solution has not moved energy as far into the problem as the transport solution. In this problem the conventional wisdom that the P_1 approximation would perform better as time passes and more particles have been absorbed and later emitted proves to be an ignis fatuus.

4. POINT SOURCE GREEN'S FUNCTION

The P_1 system given by Eqs. (10-13) is linear and rotationally invariant. This means we can use the following transform to construct the Green's function for a point source

$$E_{\text{point}}(r,t) = -\frac{1}{2\pi r}\left.\frac{\partial E_{\text{plane}}}{\partial x}\right|_{x=r} \qquad r > 0. \quad (19)$$

Upon using this transform, the solution for a point source at the origin becomes

$$E_{\text{point}}(r,\tau) = -\frac{\sqrt{3}}{4\pi r}e^{-\tau}\frac{\partial}{\partial r}\left(\frac{\tau I_1(\sqrt{\tau^2-3r^2})}{\sqrt{\tau^2-3r^2}}h(\tau-\sqrt{3}r) + I_0(\sqrt{\tau^2-3r^2})\delta(\tau-\sqrt{3}r)\right) \quad (20)$$

We point out to the reader that the derivative of a delta function will result in a negative energy density in certain regions of the problem.

5. LINE SOURCE

To get the line source we can integrate the point source, Eq. (20), in the following transform

$$G_{\text{line}}(\rho,\tau) = 2\int_0^\infty dz G_{\text{point}}(\sqrt{\rho^2+z^2},\tau). \quad (21)$$

where $r \to \sqrt{z^2+\rho^2}$.

To begin this computation we will change the variable of integration from z to r. This change gives

$$dr = \frac{zdz}{\sqrt{z^2+\rho^2}} \quad (22)$$

$$z = \sqrt{r^2-\rho^2} \quad (23)$$

$$dz = \frac{\sqrt{z^2+\rho^2}dr}{z} = \frac{rdr}{3\sqrt{r^2-\rho^2}}. \quad (24)$$

The limits of integration are also changed. The lower limit becomes $r = \rho$ while the upper limit remains infinite. Our point to line transform is then

$$G_{\text{line}}(\rho,\tau) = 2\int_\rho^\infty dr\frac{r}{\sqrt{r^2-\rho^2}}G_{\text{point}}(r,\tau). \quad (25)$$

Substituting Eq. (20) into the transform in Eq. (25) yields the integral we must compute to find the energy density due to the line source

$$G_{\text{line}}(\rho,\tau) = \sqrt{3}e^{-\tau}\int_\rho^\infty dr\frac{-1}{2\pi\sqrt{r^2-\rho^2}}\frac{\partial}{\partial r}\left(\frac{\tau I_1(\sqrt{\tau^2-3r^2})}{\sqrt{\tau^2-3r^2}}h(\tau-\sqrt{3}r) + I_0(\sqrt{\tau^2-3r^2})\delta(\tau-\sqrt{3}r)\right). \quad (26)$$

We will first handle the term with the delta function that represents the uncollided particles

$$\int_\rho^\infty dr\frac{-1}{2\pi\sqrt{r^2-\rho^2}}\frac{\partial}{\partial r}\left(I_0(\sqrt{\tau^2-3r^2})\delta(\tau-\sqrt{3}r)\right). \quad (27)$$

The derivative part of the integral can be expanded to

$$\frac{\partial}{\partial r}\left(I_0(\sqrt{\tau^2-3r^2})\delta(\tau-\sqrt{3}r)\right) = -3r\delta(\tau-\sqrt{3}r)\frac{I_1(\sqrt{\tau^2-3r^2})}{\sqrt{\tau^2-3r^2}} - \sqrt{3}I_0(\sqrt{\tau^2-3r^2})\delta'(\tau-\sqrt{3}r). \quad (28)$$

This can be related to a time derivative by noticing that

$$\frac{\partial}{\partial \tau}\left(I_0(\sqrt{\tau^2-3r^2})\delta(\tau-\sqrt{3}r)\right) = \tau\delta(\tau-\sqrt{3}r)\frac{I_1(\sqrt{\tau^2-3r^2})}{\sqrt{\tau^2-3r^2}} + I_0(\sqrt{\tau^2-3r^2})\delta'(\tau-\sqrt{3}r) \quad (29)$$
$$= \sqrt{3}r\delta(\tau-\sqrt{3}r)\frac{I_1(\sqrt{\tau^2-3r^2})}{\sqrt{\tau^2-3r^2}} + I_0(\sqrt{\tau^2-3r^2})\delta'(\tau-\sqrt{3}r),$$

where in the second equality we have used the fact that due to the delta function we can replace t with $\sqrt{3}r$. Using Eqs. (28) and (29) we now have that

$$-\sqrt{3}\frac{\partial}{\partial t}I_0(\sqrt{\tau^2-3r^2})\delta(\tau-\sqrt{3}r) = \frac{\partial}{\partial r}I_0(\sqrt{\tau^2-3r^2})\delta(\tau-\sqrt{3}r). \quad (30)$$

The relation in Eq. (30) changes our integral to

$$\frac{\partial}{\partial \tau}\int_\rho^\infty dr\frac{\sqrt{3}}{2\pi\sqrt{r^2-\rho^2}}\,I_0(\sqrt{\tau^2-3r^2})\delta(\tau-\sqrt{3}r) = \frac{\partial}{\partial \tau}\left(\frac{\sqrt{3}}{2\pi\sqrt{\tau^2-3\rho^2}}h(\tau-\sqrt{3}\rho)\right). \quad (31)$$

We now expand the derivative in the step function term of Eq. (26),

$$\int_\rho^\infty dr\frac{-1}{2\pi\sqrt{r^2-\rho^2}}\frac{\partial}{\partial r}\left(\frac{\tau I_1(\sqrt{\tau^2-3r^2})}{\sqrt{\tau^2-3r^2}}h(\tau-\sqrt{3}r)\right) = \quad (32)$$
$$\int_\rho^\infty dr\frac{-1}{2\pi\sqrt{r^2-\rho^2}}\left[\frac{-\sqrt{3}\tau I_1(\sqrt{\tau^2-3r^2})}{\sqrt{\tau^2-3r^2}}\delta(\tau-\sqrt{3}r) + h(\tau-\sqrt{3}r)\frac{\partial}{\partial r}\left(\frac{\tau I_1(\sqrt{\tau^2-3r^2})}{\sqrt{\tau^2-3r^2}}\right)\right].$$

The first term on the RHS of Eq. (32) simplifies to

$$\int_\rho^\infty dr\frac{-1}{2\pi\sqrt{r^2-\rho^2}}\left[\frac{\sqrt{3}\tau I_1(\sqrt{\tau^2-3r^2})}{\sqrt{\tau^2-3r^2}}\delta(\tau-\sqrt{3}r)\right] = \frac{-\sqrt{3}\tau}{4\pi\sqrt{\tau^2-3\rho^2}}h(\tau-\sqrt{3}\rho). \quad (33)$$

The solution from a line source is then

$$G_{\text{line}}(\rho,\tau) = \sqrt{3}e^{-\tau}\left[\frac{\partial}{\partial \tau}\left(\frac{\sqrt{3}}{2\pi\sqrt{\tau^2-3\rho^2}}h(\tau-\sqrt{3}\rho)\right) + \frac{\sqrt{3}\tau}{4\pi\sqrt{\tau^2-3\rho^2}}h(\tau-\sqrt{3}\rho)\right. \quad (34)$$
$$\left. + \int_\rho^\infty dr\frac{-1}{2\pi\sqrt{r^2-\rho^2}}\,h(\tau-\sqrt{3}r)\frac{\partial}{\partial r}\left(\frac{\tau I_1(\sqrt{\tau^2-3r^2})}{\sqrt{\tau^2-3r^2}}\right)\right] \quad (35)$$

The integrals of Bessel functions over a finite domain must be evaluated numerically. These integrals need to be evaluated carefully due to the fact that there is a square-root singularity at the lower endpoint.

We will compare this solution to a state-of-the art spherical harmonics code for radiative transfer developed by the authors [7]. Using the line source we can compare numerical results from $x-z$ geometry to an analytic solution. These numerical solutions are compared to the solution derived above in Fig. 3. This problem is quite difficult to solve numerically early in time. This is due to several issues; firstly, simulating a delta function numerically is difficult. Moreover, the temperature source is localized near the center of the problem early in time. These factors cause the numerical solution to converge very slowly to the analytic solution.

In the analytic solution we notice that behind the delta function there is a region of negative energy density. This negativity decays as the delta function decays. At $\tau = 10$ the negative region has disappeared.

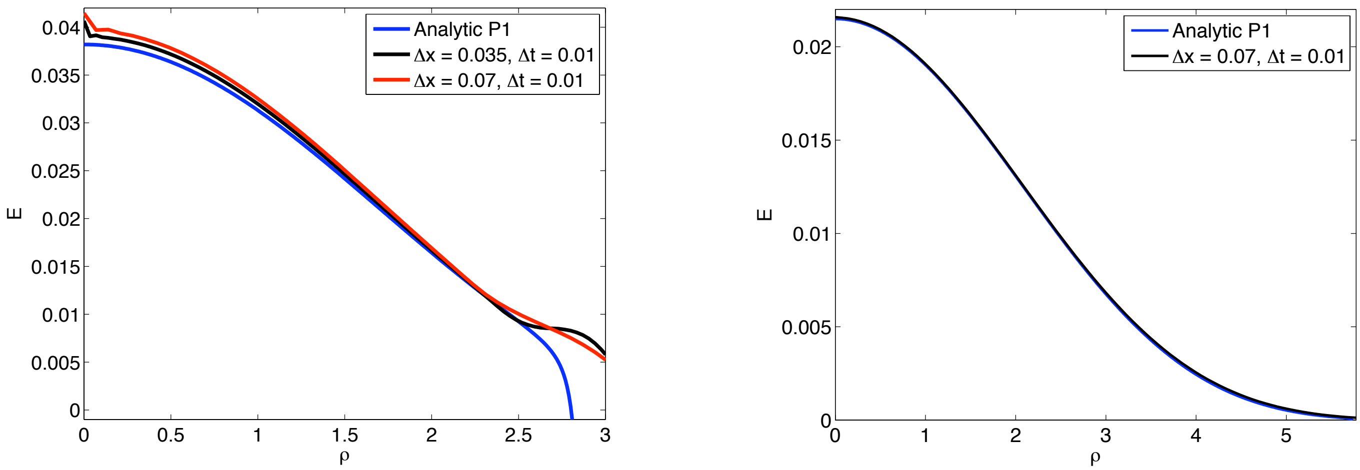

(a) $t = 5$

(b) $t = 10$

Figure 3. Line out comparison between numerical and analytic solutions. The analytic solution shows only the collided energy density, while the numerical solution is both the collided and uncollided solution.

6. CONCLUSION

We have presented benchmark solutions for the P_1 equations in various geometries. The slab geometry Green's function was used to construct a P_1 solution to one of the Su-Olson benchmarks. Comparisons between the analytic transport and P_1 solutions showed that the P_1 was best early in time. Later in time the P_1 solution was too low in the source region and placed too much energy outside the source. Also, the slow wavespeed of P_1 placed the wavefront at the wrong place.

The point source Green's function was also derived and then used to create a pulse line source solution. Having the point source Green's function we can, in principle, construct any shape of source in an infinite medium that we desire. At present the authors are attempting to construct a two-dimensional square source to give an even more useful benchmark for 2D P_n codes.

REFERENCES

[1] G.C. Pomraning. The non-equilibrium Marshak wave problem. *J. Quantitative Spectroscopy and Radiative Transfer*, 21:249–261, 1979.

[2] Bingjing Su and Gordon L. Olson. Benchmark results for the non-equilibrium Marshak diffusion problem. *J. Quantitative Spectroscopy and Radiative Transfer*, 56(3):337–351, 1996. Diffusion Benchmark.

[3] I. R. Shokair and G. C. Pomraning. Boundary conditions for differential approximations. *J. Quantitative Spectroscopy and Radiative Transfer*, 25:325, 1981.

[4] B.D. Ganapol and G. C. Pomraning. The non-equilibrium marshak wave problem: A transport theory solution. *J. Quantitative Spectroscopy and Radiative Transfer*, 29:311, 1983.

[5] Bingjing Su and Gordon L. Olson. An analytic benchmark for non-equilibrium radiative transfer in an isotropically scattering medium. *J. Quantitative Spectroscopy and Radiative Transfer*, 24(13):1035–1055, 1997.

[6] R. Paul Drake. *High-Energy-Density Physics: Fundamentals, Inertial Fusion, and Experimental Astrophysics*. Springer, 2006.

[7] Ryan G. McClarren, James Paul Holloway, Thomas A. Brunner, and Thomas A. Mehlhorn. A quasi-linear implicit Riemann solver for the time-dependent P_n equations. *Nucl. Sci. and Eng.*, 155:290–299, 2007.

[8] Ryan G. McClarren, James Paul Holloway, and Thomas A. Brunner. An upwind spherical harmonics method for thermal radiation transfer. In *Transactions of the American Nuclear Society*, volume 95, pages 879–880, La Grange Park, Illinois, 2006. American Nuclear Society.

[9] Milton Abramowitz and Irene A. Stegun. *Handbook of Mathematical Functions with Formulas, Graphs, and Mathematical Tables*. Dover, New York, ninth dover printing, tenth gpo printing edition, 1964.